Flow bifurcations for an SU(1,1) kicked top in the semiclassical representation

1993 J. Phys. A: Math. Gen. 26 6251

(http://iopscience.iop.org/0305-4470/26/22/024)

J. Phys. A: Math. Gen. 26 (1993) 6251–6260. Printed in the UK

Flow bifurcations for an $SU(1, 1)$ kicked top in the semiclassical representation

E S Hernandez and D M Jezek

Departamento de Fisica, Facultad de Ciencias Exactas y Naturales, Universidad de Buenos Aires, 1428 Buenos Aires, Argentina

Received 2 March 1993, in final form 6 July 1993

Abstract. In the spirit of establishing analogies and diferences among systems with $SU(1, 1)$ and $SU(2)$ algebras, we study the motion of an $SU(1, 1)$ kicked top in the semiclassical approximation as given by the coherent states representation. For this sake, we have proposed a Hamiltonian with the same algebraic structure as the one studied by Haake *et al* for the $SU(2)$ case, so as to investigate the modifications undergone by the phase portrait when changing a compact into a non-compact manifold. Analogously to the problem discussed by Haake *et al*, we obtain one involution and the associated symmetry line where fixed points lie; however, in contrast with the $SU(2)$ case, there exists an infinite number of solutions for every set of parameters. When increasing the strength of the kick no new stationary points are born; instead, existing fixed points simply move towards the vertex of a curve and eventually, two of them merge together and annihilate. No other type of bifurcation is detected.

1. Introduction

Forced systems have periodically attracted generous attention among theorists in the field of nonlinear dynamics. In particular the kicked rotator has become a paradigm [1] of a mobile exhibiting both regular and chaotic motion in the classical limit, as well as an important tool with which to investigate the characteristics and scope of quantum chaos [2].

Among several approaches a special realization of a quantum kicked top has been examined by Haake [2]. A major feature of the model proposed in [2] and of the technology developed to carry out the analysis of the motion resides in the extensive use of the algebraic and topological properties of angular momentum operators. In fact, the time-dependent Hamiltonian that accounts for a periodic sequence of impulses perturbing a free spin precession is a quadratic function of the $SU(2)$ algebra generators. Due to this structure, the Hamiltonian belongs to a class whose time-independent version has been intensively investigated [3, 4] in the semiclassical representation, which gives rise to a nonlinear Euler-like equation of motion on the sphere capable of exhibiting structural instabilities [5]. More recently, it has been shown [6] that semiclassical descriptions of pseudospin systems with quadratic Hamiltonians can be analysed with the previous methods. In this frame, a pseudospin operator is the vector $\hat{\boldsymbol{K}} = (\hat{k}_1, \hat{k}_2, \hat{k}_3)$ of the $SU(1, 1)$ algebra generators; since the corresponding Lie group manifold is non-compact, the index of a curve [7] is not necessarily conserved under a bifurcation. Consequently, the semiclassical phase flow possesses a richer structure than for quasispin $SU(2)$ systems, since the total number of fixed points is not a constant.

Since $SU(1, 1)$ Hamiltonian models present a large variety of physical realizations (see for example [8–10]), especially in quantum optics and many-body problems, we believe that

0305-4470/93/226251+10$07.50

a natural byproduct of this prior work [6] is to investigate the main characteristics of the stroboscopic map for a kicked system. Indeed, Gerry *et al* [11] have recently investigated the regular and stochastic motion of a pulsating $SU(1, 1)$ model aimed at representing squeezed vacuum states in a nonlinear optical environment. In this work, the traces of classical chaos are weak in the quantum version. In view of this result, rather than attempting a comparison between the classical and the quantum dynamics, in the present paper we are particularly concerned with learning about the type of bifurcation that the classical phase flow may undergo when the kicking strength is varied [5, 6], as compared with the equivalent $SU(2)$ model.

With this in mind, we present a model for a kicked $SU(1, 1)$ top similar to that in [2] and consider the map associated with the nonlinear Bloch equation for the pseudospin vector [6] in the presence of the pulsating perturbation. This is the subject of section 2. In section 3, we examine the simplest symmetries of the map and the evolution in parameter space is illustrated by a numerical example in section 4. The contents of this paper are summarized in section 5.

2. Derivation of the map

We consider a kicked system with $SU(1, 1)$ spectrum generating algebra for the unperturbed motion, the generators being the components $\hat{k}_i$ of the pseudospin vector $\hat{K}$ satisfying the conmutation relations

$$[\hat{k}_1, \hat{k}_2] = -\mathrm{i}\hat{k}_3 \tag{1}$$

$$[\hat{k}_2, \hat{k}_3] = \mathrm{i}\hat{k}_1 \tag{2}$$

$$[\hat{k}_3, \hat{k}_1] = i\hat{k}_2. \tag{3}$$

The Casimir operator is

$$\hat{C} = \hat{k}_3^2 - \hat{k}_1^2 - \hat{k}_2^2 \tag{4}$$

with eigenvalue $k(k-1)$ in the Bargmann representation $|k, n\rangle$ [12]. Following Haake [2] we select the Hamiltonian

$$\hat{H}(t) = \frac{p}{\tau}\hat{k}_2 + \alpha\hat{k}_3^2 \sum_{n=-\infty}^{\infty} \delta(t - n\tau) \tag{5}$$

where τ is the period of the pulsating perturbation and p, α strength parameters.

It is well known in the theory of kicked systems [2, 11, 13] that the mapping for times $n\tau$ is achieved by operating on state vectors and observables with the quantum propagator

$$U(n\tau, 0) = U(\tau, 0)^n \tag{6}$$

where the one-step evolution splits into a free propagation between kicks multiplied by a jump through the perturbation, i.e.

$$U(\tau, 0) = \exp(-\mathrm{i}\alpha\hat{k}_3^2)\exp(-\mathrm{i}p\hat{k}_2). \tag{7}$$

In the present study we restrict ourselves to the semiclassical map obtained from the action of the evolution operator (7) on an $SU(1, 1)$ coherent state $|z\rangle$ defined as [14]

$$|z\rangle = \exp(z\hat{k}_+ - z\hat{k}_-)|k, 0\rangle \tag{8}$$

where $\hat{K}_\pm = \hat{k}_1 \pm \hat{k}_2$ and $z = \tanh(\frac{1}{2}\theta e^{-i\phi})$. These states are in one-to-one correspondence with points in the upper branch of a two-sheeted hyperboloid in a three-dimensional space $\boldsymbol{K} = (k_1, k_2, k_3)$ with $k_i = \langle z|\hat{k}_i|z\rangle$ (see, for example, [6] and references therein); this quadric is defined by

$$C(\boldsymbol{K}) = k_3^2 - k_1^2 - k_2^2 = k \qquad k_3 > k > 0. \tag{9}$$

This is due to an essential property of coherent states of the $SU(1, 1)$ group, namely the factorization relationship [6],

$$\langle z|1/2[\hat{k}_i, \hat{k}_j]_+|z\rangle = \frac{2k+1}{2k} k_i k_j - \Delta_i \delta_{ij} \tag{10}$$

where $[\,,\,]_+$ denotes the anticommutator and $\Delta_1 = \Delta_2 = -\Delta_3 = -\frac{1}{2}k$.

Accordingly, we consider that the pseudospin motion takes place on the manifold (9) at any time; in such a case, for any Hamiltonian $\hat{H}(\boldsymbol{K})$, the variational principle leads to a classical equation of motion [6],

$$\dot{\boldsymbol{K}} = -\tfrac{1}{2}\nabla H \times \nabla C \tag{11}$$

with

$$H(\boldsymbol{K}) = \langle z|\hat{H}|z\rangle \tag{12}$$

and C given by (9). Considering (5) and (10), one obtains

$$H(\boldsymbol{K}) = \frac{p}{\tau} k_2 + \alpha \frac{2k+1}{2k} k_3 \sum_{n=-\infty}^{\infty} \delta(t - n\tau) \tag{13}$$

thus

$$\dot{\boldsymbol{K}} = \left(\left(\frac{p}{\tau} + 2\chi(t)k_2\right) k_3, -2\chi(t)k_1 k_3, \frac{p}{\tau} k_1\right) \tag{14}$$

with

$$\chi(t) = \frac{2k+1}{2k} \alpha \sum_{n=-\infty}^{\infty} \delta(t - n\tau). \tag{15}$$

The equation of motion (14) can be integrated as follows. One realizes that for $(n-1)\tau < t < n\tau$, the pulsating perturbation is not active; the time variation of the pseudospin is the free one,

$$\dot{k}_1 = (p/\tau)k_3 \tag{16}$$

$$\dot{k}_2 = 0 \tag{17}$$

$$\dot{k}_3 = (p/\tau)k_1. \tag{18}$$

Calling τ_+ and τ_- the times just after and just before the kick that takes place in $t = n\tau$, and τ_0 the time after the kick in $t = (n-1)\tau$, one readily gets the unitary map

$$k_1(\tau_-) = k_1(\tau_0)\cosh p - k_3(\tau_0)\sinh p \tag{19}$$

$$k_2(\tau_-) = k_2(\tau_0) \tag{20}$$

$$k_3(\tau_-) = -k_1(\tau_0)\sinh p + k_3(\tau_0)\cosh p. \tag{21}$$

Now during the kick, say between τ_- and τ_+, the pseudospin jumps according to

$$\dot{k}_1 = 2\chi(t)k_2k_3 \tag{22}$$

$$\dot{k}_2 = -2\chi(t)k_1k_3 \tag{23}$$

$$\dot{k}_3 = 0 \tag{24}$$

and it is worthwhile noticing that either dynamical system (16)–(18) or (22)–(24) preserves the manifold definition (9), i.e. both are maps of the hyperboloidal sheet onto itself.

Equations (22)–(24) cannot be straightforwardly integrated in spite of the appearance of the Dirac's delta in $\chi(t)$, since the values of the components k_1 and k_2 of $\boldsymbol{K}(t)$ at $t = n\tau$ are indeterminate, so we found that it is convenient to work in polar coordinates

$$\boldsymbol{K} = k(\cos\phi\sin\theta, \sin\phi\sin\theta, \cos\theta). \tag{25}$$

It is clear from (22)–(24) that $\boldsymbol{K}$ moves in a circle in the (k_1, k_2) plane; in particular it is verified that $k_1\dot{k}_1 + k_2\dot{k}_2 = 0$. Replacing (25) on (22)–(24) we obtain

$$\dot{\phi} = 2\chi(t)k_3 \tag{26}$$

which leads directly to

$$\phi(\tau_+) = 2\chi k_3 + \phi(\tau_-) \tag{27}$$

with $\chi = \alpha(2k+1)/2k$, and so, finally,

$$k_1(\tau_+) = k\cos(\phi(\tau_+)) = \cos(2\chi k_3)k_1(\tau_-) - \sin(2\chi k_3)k_2(\tau_-) \tag{28}$$

$$k_2(\tau_+) = k\sin(\phi(\tau_-)) = \cos(2\chi k_3)k_2(\tau_-)) + \sin(2\chi k_3)k_1(\tau_-). \tag{29}$$

The full map between τ_0 and τ_+ is then the composition of (28)–(29) and (19)–(21), actually

$$k_1' = (k_1\cosh p - k_3\sinh p)\cos(2\chi k_3') - k_2\sin(2\chi k_3') \tag{30}$$

$$k_2' = (k_1\cosh p - k_3\sinh p)\sin(2\chi k_3') + k_2\cos(2\chi k_3') \tag{31}$$

$$k_3' = -k_1\sinh p + k_3\cosh p \tag{32}$$

with the abridged notation $k_i' = k_i(\tau_+)$ and $k_i = k_i(\tau_0)$. It is worthwhile noticing that this procedure applied to the kicked $SU(2)$ top yields precisely the equations of motion on the sphere derived by resorting to the one-step propagator [1].

It is interesting to note that, even though a transformation such as equation (25) could not be written, equation (7) shows that the dynamics can be interpreted as generated by two time-independent Hamiltonians acting during disjoint periods τ_1 and τ_2 with $\tau_1 + \tau_2 = \tau$. For each choice of the decomposition intervals, the subsequent equations of motion may be straightforwardly integrated.

3. Symmetries and invariant points

The set of equations (30)–(32) represent a nonlinear area-preserving map

$$\boldsymbol{K}' = F(\boldsymbol{K})\boldsymbol{K} \tag{33}$$

with unitary matrix

$$F(\boldsymbol{K}) = \begin{vmatrix} \cosh p \cos(2\chi k_3') & -\sin(2\chi k_3') & -\sinh p \cos(2\chi k_3') \\ \cosh p \sin(2\chi k_3') & \cos(2\chi k_3') & -\sinh p \sin(2\chi k_3') \\ -\sinh p & 0 & \sinh p \end{vmatrix}. \tag{34}$$

It is now possible to verify that the linear transformation $T\boldsymbol{K}$, with T defined by

$$T = \begin{vmatrix} -\cosh p & 0 & \sinh p \\ 0 & 1 & 0 \\ -\sinh p & 0 & \cosh p \end{vmatrix} \tag{35}$$

satisfies the following set of conditions:

(i) $T^2 = I$, with I the 3×3 identity matrix;
(ii) $\det T = -1$;
(iii) $TFT = F^{-1}$, where the inverse transformation F^{-1} is the time-reverse one $F(-\tau)$.

Following the procedure employed by Haake *et al* [2] to locate periodic orbits and fixed points of the map using involutions, one can, in particular, define the so-called T-line, namely the symmetry line

$$T\boldsymbol{K} = \boldsymbol{K}. \tag{36}$$

One finds the plane

$$k_1 = \frac{\sinh p}{\cosh p + 1} k_3. \tag{37}$$

Equation (37) simply says that as the kick conserves the value of k_3, a fixed point must verify that the rotation around k_2 also leaves k_3 (see equation (21)) invariant.

Furthermore, setting $k = 1$, the fixed points $\boldsymbol{K}_0 = F(\boldsymbol{K}_0)$ satisfy the relation

$$f(x, \chi) = \left(1 - \frac{v^2}{\sin(x/2)^2}\right) x^2 - 4\chi^2 = 0 \tag{38}$$

with $x = 2\chi k_3$ and $v = (\cosh(p) - 1)/\sinh(p)$.

When χ is small, for low values of x, equation (38) may be approximated by

$$x = \sqrt{4v^2 + (2\chi)^2} \tag{39}$$

and for large x

$$x = 2\sin^{-1}(\pm v). \tag{40}$$

Equation (39) has a single solution, $k_3 = \sqrt{(v/\chi)^2 + 1} > 1$, while (40) gives an infinite number of fixed points (v is always less than one). When increasing the parameter χ these points move towards the vertex of the curve

$$k_3 = \sqrt{\frac{1 + k_2^2}{1 - v^2}} \tag{41}$$

given by the intersection of the hyperboloid with the plane in equation (37). Note that as v does not depend on χ the values of x do not change when varying it. Morover, it is easy to obtain this result from the geometrical viewpoint. Indeed, for large values of k_3 the manifold may be visualized as a cone $k_3^2 = k_1^2 + k_2^2$ and the fixed points lie in the intersection with the plane (37), i.e. $k_1 = vk_3$. One may convince oneself that the free precession around k_2 leaves points on the intersection with invariant k_3 and switches k_1 to $k_1' = -k_1$. On the other hand, the kick is in charge of returning the latest to the original k_1. A simple geometrical construction in the (k_2, k_1) plane shows that the above condition can only take place if $\sin(\chi k_3) = k_1/k_3 = v$.

When χ is increased the character of the fixed points changes for values of x and χ encountered by solving $f(x, \chi) = 0$ together with $f'(x, \chi) = 0$, that is equation (38) and

$$x^2 v^2 \frac{\cos(x/2)}{\sin(x/2)^3} + \left(1 - \frac{v^2}{\sin(x/2)^2}\right) 2x = 0. \tag{42}$$

The left-hand side of the last equation is a rapidly oscillating function, thus in principle one may have an infinite set of solutions. Replacement of each root in equation (38) yields a critical value χ.

Moreover, if we work on variables x and χ from equation (38) it may be seen that, when increasing χ, the function $f(x, \chi)$ shifts down; if we study the second derivative of $f(x, \chi)$ with respect to x in the bifurcation points (i.e. for points that verify (42)), using (38) it is easy to obtain the expression:

$$f^{(2)}(x, \chi) = -1/2 \frac{(v \cos(x/2)x)^2}{\sin(x/2)^4} \left(3 + \left(\frac{\sin(x/2)}{\cos(x/2)} - \frac{3}{x}\right)^2 - (3/x)^2\right) \tag{43}$$

so we can assert that for values of $x > \sqrt{3}$ the critical points correspond to maxima. Taking these two characteristics into account, we conclude that, for values of x that verify the last condition, the type of bifurcation that occurs is the annihilation of a pair of points.

Other involutions $(TF)^n$ give rise to a large collection of sequences of fixed points. Due to the impossibility of classifying the latter in a systematic manner, we shall illustrate, in the next section, the evolution of the Poincaré sections as one chooses a path in parameter space.

4. Numerical results

We have iterated the map (30)–(32) for several choices of the parameters p and χ. A typical path that illustrates the features discussed at the end of the preceding section consists of choosing a value $p = 0.5$, which in turn yields $v = 0.2449$, and varying χ. In figure 1 we show the phase diagram projected on (*a*) the plane (k_1, k_3) and (*b*) the plane (k_2, k_3), for $\chi = 0.1$. We see that it presents a regular region around the fixed point $K = (0.65, 2.35, 2.64)$, whose coordinates correspond to equation (39). In figure 2 we show the same diagrams as in figure 1 for a larger value $\chi = 0.25$. It may be seen that the flux becomes more irregular and the fixed point drifts towards $K = (0.35, 0.95, 1.42)$. It should be noticed that, according to equation (41), the lowest attainable value of k_3 for a fixed point—namely the vertex of the intersection curve—is around 1.03. Up to our precision, for $\chi = 1$ the fixed point has already reached the vertex whose cordinates are (0.25, 0, 1.03); for this value of χ, other fixed points have appeared which may be calculated using equation (40). In this case, the islands that appear in figure 3 between $1.4 < k_3 < 1.8$

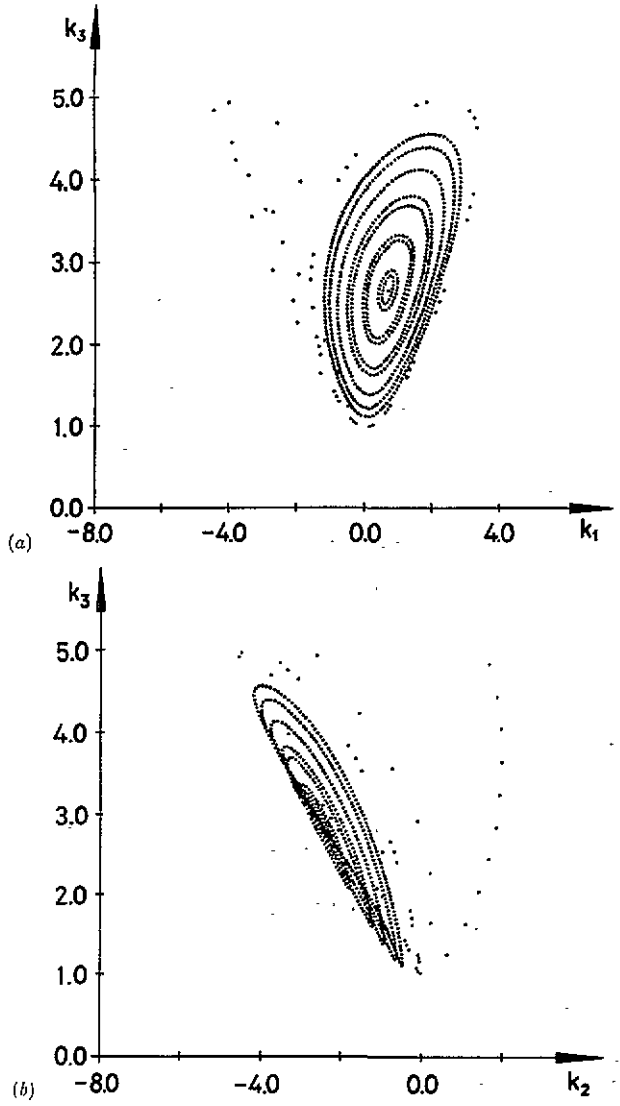

Figure 1. (*a*) Projection of the phase portrait on the plane (k_1, k_3) for $p = 0.5$ and $\chi = 0.1$; (*b*) phase portrait projection on the plane (k_2, k_3) for $p = 0.5$ and $\chi = 0.1$.

correspond to fixed points of F^2. For larger values of χ, the area of the region of irregular motion increases and the islands become too tiny, almost resembling isolated points; the Poincaré map is then of limited interest. Such behaviour when increasing the intensity of the kick is due to the accumulation of fixed points.

In table 1 we show the values of k_3 and χ for the solutions of equation (42) together with (38).

In the asymptotic limit $x \gg 1$ the largest contribution $f'(x, \chi)$ in equation (42) comes from the first term; then the roots in the given equation correspond to $\chi k_3 = x/2 = (2n + 1)\pi/2$. Equation (38) yields the coordinate χ in the bifurcation set, namely $\chi = \sqrt{1 - v^2}(2n + 1)\pi/2$ from where we finally obtain $k_3 = (1 - v^2)^{-1/2}$ for the critical points on the manifold.

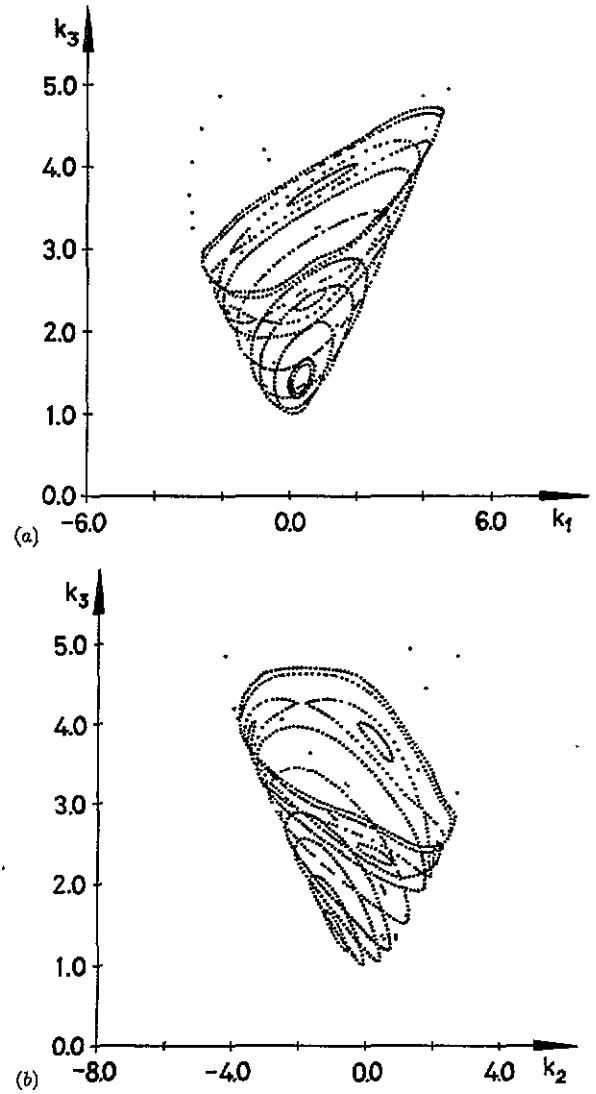

Figure 2. (*a*) Same as figure 1(*a*) for $\chi = 0.25$; (*b*) same as figure 1(*b*) for $\chi = 0.25$.

From table 1 it could be seen that, within our precision, the last two lines already correspond to the asymptotic limit. Further excursions on χ are then irrelevant.

By inspecting the first column of this table it is obvious that the condition written below equation (43) holds for all values of x, so we conclude that the type of phase transition that occurs is the merging of two critical points into none.

In other words, when increasing the strength of the kick the critical points move toward the vertex of the curve given by equation (41) and collapse in pairs near the vertex. It is clear that though the manifold is not compact it does not possess an associated characteristic; however, the sum of the indices of the critical points involved in a bifurcation remains constant.

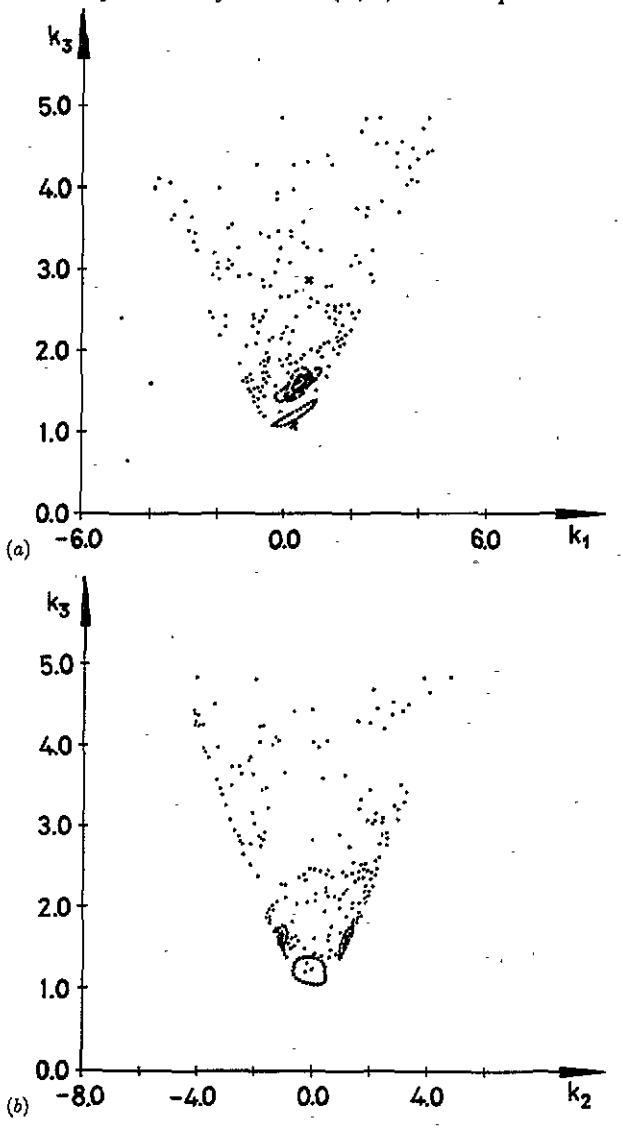

Figure 3. (*a*) Same as figure 1(*a*) for $\chi = 1$; (*b*) same as figure 1(*b*) for $\chi = 1$.

Table 1. *The first column corresponds to the solutions of equation (42), while in the second* and third columns we show the kick strength parameter and the k_3 coordinate of the bifurcation points, respectively.

χk_3	χ	k_3
5.56	2.29	2.42
8.6	8.11	1.06
11.7	11.08	1.05
14.7	14.07	1.04
17.8	17.07	1.04
20.9	20.09	1.04
24	23.1	1.03
27.1	26.12	1.03

5. Summary

In this work we have attempted to push one step forward in the field of semiclassical descriptions of the motion for systems with spectrum generating algebras, so as to make room for time-dependent Hamiltonians that contain a periodic sequence of kicks. As a first contribution in this direction, we have investigated the simplest generalization of the $SU(2)$ kicked top in [2], just replacing quasispin operators $\boldsymbol{J}$ by pseudospin operators $\boldsymbol{K}$. We have insisted on the picture presented in previous work concerning the dynamics on nonlinear manifolds, through nonlinear Euler- or Bloch-like equations of motion, and have constructed a strosboscopic map on the nonlinear and non-compact phase space associated with the $SU(1,1)$ group manifold. The advantage of the method employed here is that it is not necessary to look for the spectral representation of the one-step evolution operator. This advantage would, however, be lost if one was interested in looking at the spectrum of quasifrequencies of the kicked motion in order to look for statistical properties and traces of quantum chaos [2, 11].

A numerical application illustrates the birth and death of fixed points in the near-vertex region of the hyperboloideal phase space. Richer phase diagrams can be obtained looking at different regions of parameter space; in view of the infinite set of involutions and related symmetry lines, it is not possible, within our current means, to present a normalized classifications of phase flow transitions.

Acknowledgments

This work was done under grant PID 97/88 from Consejo Nacional de Investigaciones Cientificas y Tecnicas (CONICET) and N0 11811 from Fundacion Antorchas, Argentina. The authors also acknowledge CONICET for partial financial support. We are also grateful to a referee who kindly reminded us that our equation (11) is a particular case of the general equation of motion satisfied by upper symbols of generators on general Kaehler manifolds [15].

References

[1] Gerry C C and Schneider T 1990 *Phys. Rev.* A **42** 1033
[2] Haake F, Kus M and Scharf R 1987 *Z. Phys.* B **65** 381
[3] Jezek D M, Hernandez E S and Solari H G 1986 *Phys. Rev.* C **34** 297
[4] Jezek D M and Hernandez E S 1987 *Phys. Rev.* C **35** 1555
[5] Vignolo C E, Jezek D M and Hernandez E S 1988 *Phys. Rev.* C **37** 506
[6] Jezek D M and Hernandez E S 1990 *Phys. Rev.* A **42** 96
[7] Arnold V J 1973 *Ordinary Differential Equations* (Cambridge, MA: MIT)
[8] Solomon A J 1971 *J. Math. Phys.* **12** 390
[9] Bishop R F and Vourdas A 1986 *J. Phys. A: Math. Gen.* **19** 2525
[10] Dattoli G, Dipace A and Torre A 1986 *Phys. Rev.* A **33** 4387
[11] Gerry C C 1991 *Phys. Rev.* A **43** 361
[12] Bargmann V 1947 *Ann. Math.* **48** 568; 1961 *Commun. Pure Appl. Math.* **14** 187
[13] Gerry C C and Vrscay E R 1989 *Phys. Rev.* A **39** 5717
[14] Perelomov A M 1972 *Commun. Math. Phys.* **26** 222
[15] Berezin F A 1975 *Commun. Math. Phys.* **40** 153